UASLP–IF–09–001
FERMILAB–Pub–09–031–E

Nuclear Dependence of Charm Production

The SELEX Collaboration

A. Blanco-Covarrubias [k], J. Engelfried [k,*], U. Akgun [m], G. Alkhazov [i], J. Amaro-Reyes [k], A.G. Atamantchouk [i,1], A.S. Ayan [m], M.Y. Balatz [f,1], N.F. Bondar [i], P.S. Cooper [d], L.J. Dauwe [n,1], G.V. Davidenko [f], U. Dersch [g,2], A.G. Dolgolenko [f], G.B. Dzyubenko [f], R. Edelstein [b], L. Emediato [p], A.M.F. Endler [c], I. Eschrich [g,3], C.O. Escobar [p,4], N. Estrada [k], A.V. Evdokimov [f], I.S. Filimonov [h,1], A. Flores-Castillo [k], F.G. Garcia [p,d], V.L. Golovtsov [i], P. Gouffon [p], E. Gülmez [a], M. Iori [o], S.Y. Jun [b], M. Kaya [m,5], J. Kilmer [d], V.T. Kim [i], L.M. Kochenda [i], I. Konorov [g,6], A.P. Kozhevnikov [e], A.G. Krivshich [i], H. Krüger [g,7], M.A. Kubantsev [f], V.P. Kubarovsky [e], A.I. Kulyavtsev [b,d], N.P. Kuropatkin [i,d], V.F. Kurshetsov [e], A. Kushnirenko [b,e], J. Lach [d], L.G. Landsberg [e,1], I. Larin [f], E.M. Leikin [h], G. López-Hinojosa [k], T. Lungov [p], V.P. Maleev [i], D. Mao [b,8], P. Mathew [b,9], M. Mattson [b], V. Matveev [f], E. McCliment [m], M.A. Moinester [j], V.V. Molchanov [e], A. Morelos [k], A.V. Nemitkin [h], P.V. Neoustroev [i], C. Newsom [m], A.P. Nilov [f,1], S.B. Nurushev [e], A. Ocherashvili [j,10], Y. Onel [m], S. Ozkorucuklu [m,11], A. Penzo [q], S.V. Petrenko [e], M. Procario [b,12], V.A. Prutskoi [f], B.V. Razmyslovich [i,13], V.I. Rud [h], J. Russ [b], J.L. Sánchez-López [k], J. Simon [g,14], A.I. Sitnikov [f], V.J. Smith [ℓ], M. Srivastava [p], V. Steiner [j], V. Stepanov [i,13], L. Stutte [d], M. Svoiski [i,13], N.K. Terentyev [i,b], I. Torres [k], L.N. Uvarov [i], A.N. Vasiliev [e], D.V. Vavilov [e], E. Vázquez-Jáuregui [k], V.S. Verebryusov [f], V.A. Victorov [e], V.E. Vishnyakov [f], A.A. Vorobyov [i], K. Vorwalter [g,15], J. You [b,d], R. Zukanovich-Funchal [p]

[a] *Bogazici University, Bebek 80815 Istanbul, Turkey*
[b] *Carnegie-Mellon University, Pittsburgh, PA 15213, U.S.A.*
[c] *Centro Brasileiro de Pesquisas Físicas, Rio de Janeiro, Brazil*
[d] *Fermi National Accelerator Laboratory, Batavia, IL 60510, U.S.A.*
[e] *Institute for High Energy Physics, Protvino, Russia*
[f] *Institute of Theoretical and Experimental Physics, Moscow, Russia*
[g] *Max-Planck-Institut für Kernphysik, 69117 Heidelberg, Germany*
[h] *Moscow State University, Moscow, Russia*
[i] *Petersburg Nuclear Physics Institute, St. Petersburg, Russia*
[j] *Tel Aviv University, 69978 Ramat Aviv, Israel*
[k] *Universidad Autónoma de San Luis Potosí, San Luis Potosí, Mexico*
[ℓ] *University of Bristol, Bristol BS8 1TL, United Kingdom*
[m] *University of Iowa, Iowa City, IA 52242, U.S.A.*
[n] *University of Michigan-Flint, Flint, MI 48502, U.S.A.*
[o] *University of Rome "La Sapienza" and INFN, Rome, Italy*
[p] *University of São Paulo, São Paulo, Brazil*
[q] *University of Trieste and INFN, Trieste, Italy*

Abstract

With data taken by SELEX, which accumulated data during the 1996-1997 fixed target run at Fermilab, we study the production of charmed hadrons on copper and carbon targets with Σ^-, p, π^-, and π^+ beams. Parameterizing the production cross section $\propto A^\alpha$, A being the atomic number, we determine α for D^+, D^0, D_s^+, $D^+(2010)$, Λ_c^+, and their respective anti-particles, as a function of their transverse momentum p_t and scaled longitudinal momentum x_F. Within our statistics there is no dependence of α on x_F for any charm species for the interval $0.1 < x_F < 1.0$. The average value of α for charm production by pion beams is $\alpha_{\text{meson}} = 0.850 \pm 0.028$. This is somewhat larger than the corresponding average $\alpha_{\text{baryon}} = 0.755 \pm 0.016$ for charm production by baryon beams (Σ^-, p).

Key words:
PACS: 13.85.Ni, 14.65.Dw, 24.85.+p

1 Introduction

The dependence of inclusive particle production on the target material is usually characterized by a power law: $\sigma_A = \sigma_N A^\alpha$, where σ_N is the nucleon cross section and σ_A the cross section for a target with atomic mass number A. Pure hard scattering without nuclear effects corresponds to $\alpha = 1$, while $\alpha < 1$ would indicate the presence of additional processes like nuclear absorption, hadronization with intrinsic components of the nucleons, etc. To distinguish between different processes and models the dependence of α on kinematic variables, like the scaled longitudinal (x_F) and transverse (p_t) momenta, is of interest.

The production of strange particles with a proton beam shows [1,2] a strong dependence of α on both x_F and p_t. Open charm production was measured [3–9] for pion and proton beams, in different ranges of x_F, for $D^\pm$, D^0, D^*, and D_s mesons, and most of the experiments just publish one average value for α (but see Fig. 4). Charmonium production as function of x_F and p_t is reported in [10–12]; prompt single and muon pair production was measured in [13–15], and prompt neutrino production assumed to be from charm decays in [16]. As summarized in [17], most measurements are compatible with $\alpha = 1$ at $x_F \sim 0$, with only small variations in open charm, but a decrease to $\alpha \sim 2/3$ for charmonium production and in the muon data as $x_F \to 1$.

Understanding the basic production and suppression mechanisms in charm hadroproduction is not only important by itself, but also for other fields like Heavy-Ion collisions (see a review [18]) and Cosmic Ray Physics, where Monte

* Corresponding author.
Email address: `jurgen@ifisica.uaslp.mx` (J. Engelfried).
[1] deceased
[2] Present address: Advanced Mask Technology Center, Dresden, Germany
[3] Present address: University of California at Irvine, Irvine, CA 92697, USA
[4] Present address: Instituto de Física da Universidade Estadual de Campinas, UNICAMP, SP, Brazil
[5] Present address: Kafkas University, Kars, Turkey
[6] Present address: Physik-Department, Technische Universität München, 85748 Garching, Germany
[7] Present address: The Boston Consulting Group, München, Germany
[8] Present address: Lucent Technologies, Naperville, IL
[9] Present address: Baxter Healthcare, Round Lake IL
[10] Present address: NRCN, 84190 Beer-Sheva, Israel
[11] Present address: Süleyman Demirel Universitesi, Isparta, Turkey
[12] Present address: DOE, Germantown, MD
[13] Present address: Solidum, Ottawa, Ontario, Canada
[14] Present address: Siemens Healthcare, Erlangen, Germany
[15] Present address: Allianz Insurance Group IT, München, Germany

Carlo simulations take into account the production of charm particles.

We present in this letter a new measurement for α in the range of $0.1 < x_F < 1$, for 14 different open charm particles and decay modes, produced by four different beam particles.

2 Experimental Apparatus

The experimental setup of the SELEX experiment is described elsewhere [19]. We point out the most important features of the setup used in this analysis. SELEX is a 3-stage magnetic spectrometer, designed for high acceptance forward ($x_F \gtrsim 0.1$) interactions. 600 GeV/c negative ($\simeq 50\,\%$ Σ^-, $\simeq 50\,\%$ π^-) and 540 GeV/c positive beam particles ($\simeq 92\,\%$ p, $\simeq 8\,\%$ π^+), individually tagged by a Transition Radiation Detector, interact in five target foils, described in Table 1. The physical properties of the target foils were measured before the installation into the experimental setup, and the thicknesses and positions were verified by measuring the positions of the primary vertices.

Table 1
Physical Properties of Materials in the Charm Production Targets region. The layout is shown in Fig. 1.

Name	Material	Thickness L [cm]	Position [cm]	A	Density ρ [g/cm^3]	λ_{int} [%]
S4	Scintillator	0.158	-7.27	–	1.03	0.20
6	Copper	0.159	-6.13	63.5	8.96	1.06
7	Copper	0.119	-4.62	63.5	8.96	0.76
8	Diamond	0.220	-3.10	12	3.25	0.82
9	Diamond	0.220	-1.61	12	3.25	0.82
10	Diamond	0.220	-0.11	12	3.25	0.82
IC1	Scintillator	0.200	2.46	–	1.03	0.25
IC2	Scintillator	0.200	2.97	–	1.03	0.25

The spectrometer had silicon strip detectors to measure the incoming beam and outgoing tracks. Momenta of particles deflected by the analyzing magnets were measured by a system of proportional wire chambers (PWCs), drift chambers and silicon strip detectors. Momentum resolution for a typical 100 GeV/c track was $\sigma_p/p \approx 0.5\,\%$. Charged particle identification was performed with a Ring Imaging Cherenkov detector (RICH) [20], which distinguished $K^\pm$ from $\pi^\pm$ up to 165 GeV/c. The proton identification efficiency was $> 95\,\%$ above proton threshold ($\approx$ 90 GeV/c). For pions reaching the RICH detector, the total mis-identification probability due to all sources of confusion was $< 4\,\%$.

Interactions in the five target foils were selected by a scintillator trigger. The trigger for charm required at least four charged tracks downstream of the targets as indicated by an interaction counter (IC1, IC2, see Fig. 1), no signal in a veto counter (S4) upstream of the targets, and at least 2 hits in a scintillator hodoscope after the second analyzing magnet. It accepted about 1/3 of all inelastic interactions. Triggered events were further tested in an on–line computational filter based on downstream tracking and particle identification information. The on–line filter selected events that had evidence of a secondary vertex from tracks completely reconstructed using the forward PWC spectrometer and the vertex silicon. This filter reduced the data size by a factor of nearly 8 at a cost of about a factor of 2 in charm yield. From a total of $15.2 \cdot 10^9$ interactions during the 1996–1997 fixed target run about 10^9 events were written to tape.

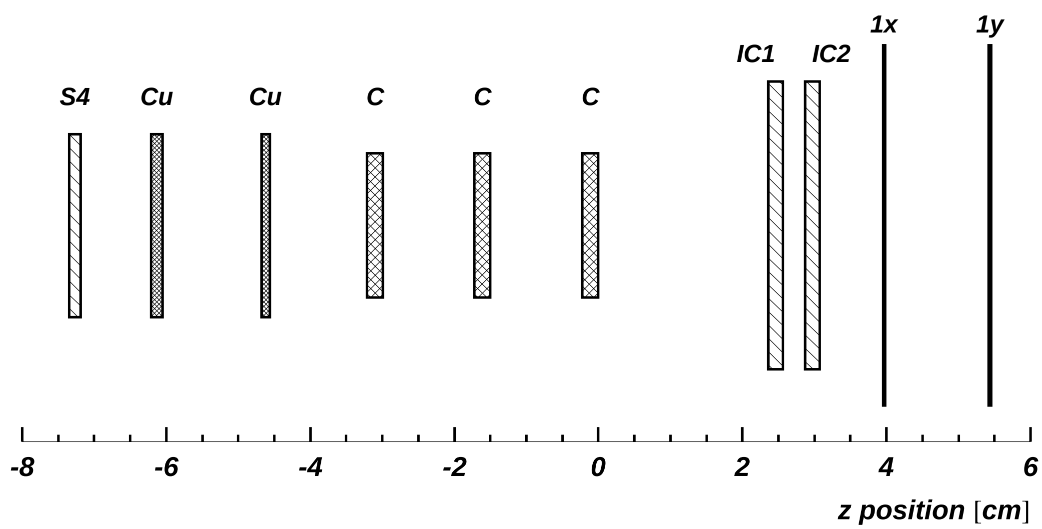

Fig. 1. Scale drawing of the charm production target region. In addition to the five targets (2 Copper, 3 Diamond) we also indicate the location of some of the scintillators used in the trigger (S4, IC1, IC2) and the first two planes (1x, 1y, from 20 in total) of the silicon strip detectors. The physical properties of the elements are shown in Table 1.

3 Data Analysis

To determine the charm production cross section dependence on the nuclear mass A, we have to determine the number of charm particles produced in any single target, and take into account the number of nuclei in the Carbon and

Copper targets. Parameterizing the cross section $\propto A^{\alpha}$, we obtain

$$\alpha = \frac{\ln\left(\frac{N_{\rm Cu}}{N_{\rm C}}\frac{\rho_{\rm C}}{\rho_{\rm Cu}}\frac{L_{\rm C}}{L_{\rm Cu}}\frac{A_{\rm Cu}}{A_{\rm C}}\right)}{\ln\left(\frac{A_{\rm Cu}}{A_{\rm C}}\right)} = \frac{\ln\frac{N_{\rm Cu}}{N_{\rm C}}}{\ln\frac{A_{\rm Cu}}{A_{\rm C}}} + \frac{\ln\left(\frac{\rho_{\rm C}}{\rho_{\rm Cu}}\frac{L_{\rm C}}{L_{\rm Cu}}\frac{A_{\rm Cu}}{A_{\rm C}}\right)}{\ln\frac{A_{\rm Cu}}{A_{\rm C}}} \quad (1)$$

with atomic masses $A_{\rm C}$, $A_{\rm Cu}$, the thicknesses $L_{\rm C}$, $L_{\rm Cu}$, and densities $\rho_{\rm C}$, $\rho_{\rm Cu}$ as shown in Table 1, and $N_{\rm C}$, $N_{\rm Cu}$ being the number of acceptance corrected events observed in the different target materials.

In this analysis, we reconstructed completely charm particles in specific decay modes. For $D^0 \to K^-\pi^+$, $D^0 \to K^-\pi^+\pi^+\pi^-$, $D^+ \to K^-\pi^+\pi^+$, $D_s^+ \to K^-K^+\pi^+$, $\Lambda_c^+ \to pK^-\pi^+$, and the corresponding charge-conjugated modes, we used cuts similar to those in previous publications [21–23]. Secondary vertex reconstruction was attempted when the χ^2 per degree of freedom for the fit of the ensemble of charged tracks to a single primary vertex exceeded 4. All combinations of tracks were formed for secondary vertices ($\chi^2_{\rm sec} < 5$) and tested against a reconstruction table that specified selection criteria for each charm decay mode. Secondary vertices which occurred inside the volume of a target were rejected. The resolution of the primary vertex position is on average better than $300\,\mu$m (depending slightly on the target foil), less than the thickness of the target foils and much less than the spacing between foils. This permits an unambiguous assignment of the interaction to a specific target foil. Additional identification criteria for the different decay modes required that proton and kaon candidate tracks were identified by the RICH detector to be at least as likely as a pion. Additionally, in the case of $D_s^{\pm} \to K^+K^-\pi^{\pm}$ for the kaon tracks the kaon hypothesis had to be more likely than the proton hypothesis. If a pion candidate track reached the RICH detector, we applied as a loose requirement that it had to have a likelihood of at least 10 %. If the track failed to reach the RICH, the candidate was called a pion. The separation between the primary and secondary vertices had to be greater than eight times its error, and the error itself less than 0.17 cm; the reconstructed charm momentum vector had to point back to the primary vertex, and two of the daughter tracks had to have a miss distance with respect to the primary vertex of more than $\sqrt{6}$ times its error. For $D^\star$ states decaying into $D^0\pi^{\pm}$, we required a reconstructed D^0 within $\pm 36\,{\rm MeV}/c^2$ ($\pm\,3$ times the resolution) of the nominal mass, and an additional pion from the primary vertex. The approximate total yields for the different modes and beam particles are shown in Table 2. The invariant mass distributions were divided into groups for the primary interaction happening in one of the target foils, and further in different x_F-bins, and in some cases also in bins of p_t^2. We used the sideband-subtraction technique to remove the background from the mass distributions. The resultant 736 different yields are the primary data for measuring α.

Table 2
Raw yields (before applying any acceptance corrections) for the charm particles and modes, for the different beam particles, used in this analysis. These yields were obtained adjusting a Gaussian and a polynomial representing the background to the invariant mass distributions.

	Decay Mode	Beam Particle Σ^-	π^-	p	π^+
1	$D^0 \to K^-\pi^+$	1176 ± 38	411 ± 22	245 ± 16	29 ± 7
2	$\overline{D^0} \to K^+\pi^-$	1740 ± 52	452 ± 23	437 ± 24	39 ± 7
3	$D^0 \to K^-\pi^+\pi^+\pi^-$	1282 ± 50	467 ± 26	252 ± 18	47 ± 6
4	$\overline{D^0} \to K^+\pi^-\pi^+\pi^-$	1650 ± 60	488 ± 29	331 ± 26	73 ± 9
5	$D^+ \to K^-\pi^+\pi^+$	1352 ± 46	361 ± 23	248 ± 20	42 ± 7
6	$D^- \to K^+\pi^-\pi^-$	2024 ± 58	555 ± 27	338 ± 22	56 ± 9
7	$D^{*+} \to D^0(K^-\pi^+)\pi^+$	165 ± 13	48 ± 7	33 ± 7	–
8	$D^{*-} \to \overline{D^0}(K^+\pi^-)\pi^-$	331 ± 20	70 ± 8	65 ± 8	–
9	$D^{*+} \to D^0(K^-\pi^+\pi^+\pi^-)\pi^+$	235 ± 15	61 ± 9	58 ± 9	–
10	$D^{*-} \to \overline{D^0}(K^+\pi^-\pi^+\pi^-)\pi^-$	446 ± 21	116 ± 11	80 ± 10	–
11	$D_s^+ \to K^-K^+\pi^+$	118 ± 17	62 ± 11	–	–
12	$D_s^- \to K^+K^-\pi^-$	379 ± 26	91 ± 12	–	–
13	$\Lambda_c^+ \to pK^-\pi^+$	1130 ± 39	172 ± 15	240 ± 16	–
14	$\overline{\Lambda_c^-} \to \overline{p}K^+\pi^-$	313 ± 34	95 ± 13	42 ± 9	–

The total acceptance (geometrical acceptance and reconstruction efficiencies) for the different decay modes of interest was estimated by embedding Monte Carlo charm decay tracks into data events. Events were generated with transverse and longitudinal momentum distributions. Detector hits, including resolution and multiple Coulomb scattering smearing effects, produced by these embedded tracks were folded into arrays of hits from real events. The new ensemble of hits was passed through the SELEX off–line software. The acceptance is the ratio of the number of reconstructed events over the number of embedded events in a particular mode for a specific target foil and bin in x_F and p_t^2. As seen from equation 1, only differences in the acceptances between the target foils are important; the largest effects depend on the lifetime of the different states. For example, for Λ_c^+ decays in the x_F interval 0.4–0.6 the acceptance varies from 21.4 % to 23.5 % between target 7 and target 10, while for D^+ decays the variation is from 41.4 % to 31.8 %. We verified our acceptance corrections by comparing the corrected event yields as functions of x_F and p_t for our three identical diamond targets and found good agreement within our statistics. This study was performed for all the

Table 3
α-values for the different charm particles and decay modes, for different beam particles. Only statistical errors are shown. We do not determine α for a specific mode and/or bin of x_F if the number of observed events is below 1.

Beam	Mode	α $0.1 < x_F < 0.2$	α $0.2 < x_F < 0.4$	α $0.4 < x_F < 0.6$	α $x_F > 0.6$
Σ^-	1	0.75 ± 0.07	0.72 ± 0.07	0.48 ± 0.25	–
Σ^-	2	0.80 ± 0.05	0.70 ± 0.06	0.98 ± 0.18	0.71 ± 1.54
Σ^-	3	0.52 ± 0.18	0.66 ± 0.09	0.57 ± 0.22	0.67 ± 0.68
Σ^-	4	0.47 ± 0.19	0.67 ± 0.09	0.80 ± 0.17	1.23 ± 0.92
Σ^-	5	0.75 ± 0.09	0.68 ± 0.07	0.33 ± 0.27	–
Σ^-	6	0.80 ± 0.08	0.79 ± 0.06	0.74 ± 0.13	0.84 ± 0.59
Σ^-	7	0.86 ± 0.24	0.89 ± 0.15	0.57 ± 0.31	–
Σ^-	8	0.63 ± 0.19	0.73 ± 0.11	0.74 ± 0.20	–
Σ^-	9	0.43 ± 0.45	0.41 ± 0.17	0.88 ± 0.17	–
Σ^-	10	0.80 ± 0.21	0.80 ± 0.10	0.84 ± 0.14	0.47 ± 0.50
Σ^-	11	1.10 ± 0.38	1.07 ± 0.19	–	–
Σ^-	12	0.99 ± 0.35	0.79 ± 0.12	0.87 ± 0.16	–
Σ^-	13	0.70 ± 0.20	0.95 ± 0.08	0.90 ± 0.10	0.83 ± 0.17
Σ^-	14	1.32 ± 0.25	0.74 ± 0.24	–	–
π^-	1	0.86 ± 0.14	0.82 ± 0.11	0.25 ± 0.24	–
π^-	2	0.89 ± 0.12	0.78 ± 0.11	0.96 ± 0.17	–
π^-	3	0.85 ± 0.32	0.87 ± 0.12	0.82 ± 0.17	1.00 ± 0.18
π^-	4	1.04 ± 0.22	0.88 ± 0.15	0.59 ± 0.19	0.75 ± 0.29
π^-	5	0.37 ± 0.34	0.70 ± 0.13	0.79 ± 0.17	1.27 ± 0.37
π^-	6	0.76 ± 0.18	0.75 ± 0.10	0.89 ± 0.16	0.83 ± 0.21
π^-	7	1.50 ± 0.56	1.17 ± 0.33	0.68 ± 0.36	–
π^-	8	0.34 ± 1.06	1.11 ± 0.24	0.77 ± 0.32	–
π^-	9	1.54 ± 0.60	0.95 ± 0.25	0.29 ± 0.46	1.00 ± 0.38
π^-	10	–	0.99 ± 0.22	0.70 ± 0.25	1.01 ± 0.22
π^-	11	–	0.42 ± 0.49	0.83 ± 0.58	–
π^-	12	–	0.87 ± 0.24	0.68 ± 0.44	1.52 ± 1.04
π^-	13	1.42 ± 0.54	1.08 ± 0.18	0.84 ± 0.27	0.80 ± 0.37
π^-	14	–	–	0.95 ± 0.37	–
p	1	0.56 ± 0.18	0.65 ± 0.14	0.76 ± 0.56	–
p	2	0.77 ± 0.12	0.67 ± 0.12	0.32 ± 0.41	–
p	3	0.77 ± 0.34	0.53 ± 0.20	0.74 ± 0.27	–
p	4	0.61 ± 0.35	0.45 ± 0.20	0.37 ± 0.54	0.93 ± 2.32
p	5	0.50 ± 0.26	0.71 ± 0.14	–	–
p	6	0.94 ± 0.18	0.80 ± 0.12	1.02 ± 0.26	–
p	7	–	0.61 ± 0.35	0.47 ± 0.66	–
p	8	–	1.03 ± 0.19	0.35 ± 0.65	–
p	9	–	–	0.48 ± 0.48	–
p	10	–	0.73 ± 0.23	0.22 ± 0.46	–
p	13	0.51 ± 0.77	0.44 ± 0.23	0.79 ± 0.22	1.03 ± 0.30
p	14	–	1.08 ± 0.80	0.78 ± 0.55	–
π^+	1	0.37 ± 0.65	1.08 ± 0.29	0.23 ± 0.65	–
π^+	2	0.68 ± 0.34	1.23 ± 0.22	0.38 ± 0.68	–
π^+	3	–	1.00 ± 0.41	0.91 ± 0.35	1.15 ± 0.88
π^+	4	–	0.74 ± 0.32	1.57 ± 0.51	–
π^+	5	1.11 ± 0.67	0.43 ± 0.38	0.58 ± 0.80	–
π^+	6	0.59 ± 0.76	0.90 ± 0.25	1.28 ± 0.33	1.03 ± 0.60

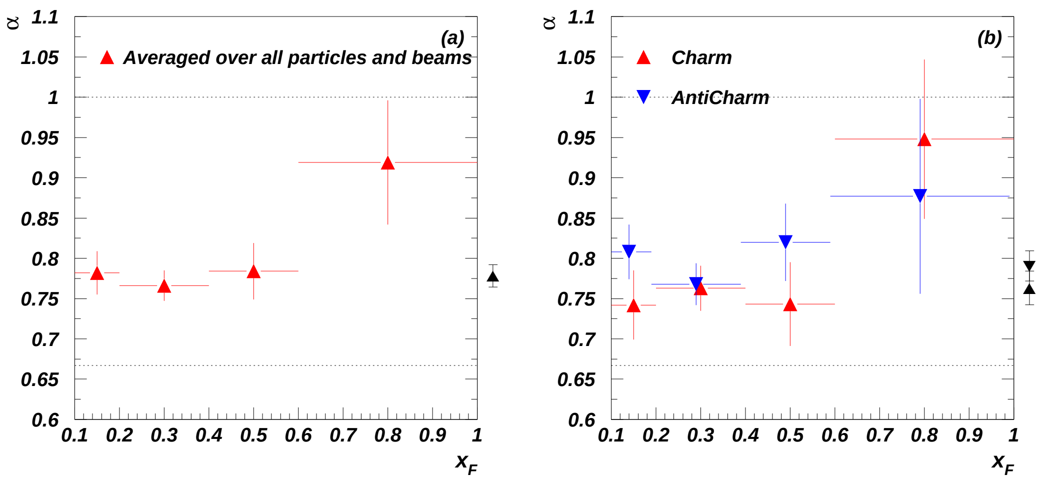

Fig. 2. Average α as function of x_F for all observed final states (a) and for charm and anti-charm (b). The data points are slightly offset to avoid overlapping of the error bars. Reference α values of 2/3 and 1 are shown as dotted lines. The points outside the frame show the average assuming that α does not depend on x_F.

charm decay modes reported here, as well as for the high statistics sample $\Lambda^0 \to p\pi^-$.

For the determination of α we use the number of observed events, corrected for acceptances, from the three diamond targets, but only from the second copper target (target number 7). Some fraction of the events with the interaction in target number 6 where vetoed in the hardware trigger by the "S4" scintillation counter due to back-splash from the interaction. In the attempt to correct for this vetoing we encountered systematic biases which would increase the combined statistical and systematic errors more than if we ignore completely the interactions from the first copper target foil.

4 Results

For any single mode, for four different beam particles, we calculated α according to equation 1. The results are presented in Table 3.

In Fig. 2(a) we show α as a function of x_F for all data, i.e., averaged over all charm and anti-charm modes and all beam particles. In Fig. 2(b) we separate the charm and anti-charm final states and show α averaged over all decay modes and beam particles for each type of charm quark.

In Fig. 3(a) we display the dependence of the average α on the beam particle type: meson or baryon. All charm and anti-charm decay modes are averaged. In Fig. 3(b) we separate the charm or anti-charm decays into leading and non-leading classes. Recall that leading charm processes are those in which the

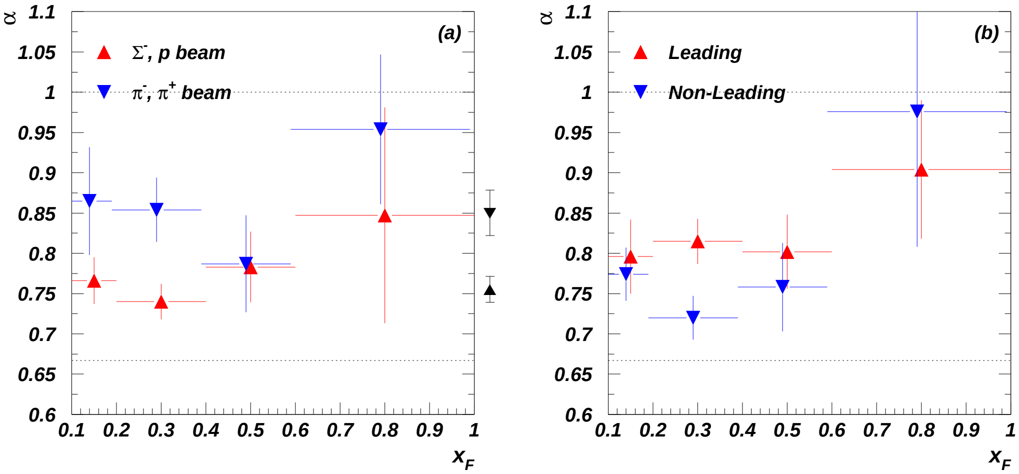

Fig. 3. Average α as a function of x_F for production by baryon (Σ^-, p) and meson ($\pi^{\pm}$) beams (a) and leading and non-leading (b) particles. The data points are slightly offset to avoid overlapping of the error bars. Reference α values of $2/3$ and 1 are shown as dotted lines. The points outside the frame show the average assuming that α does not depend on x_F.

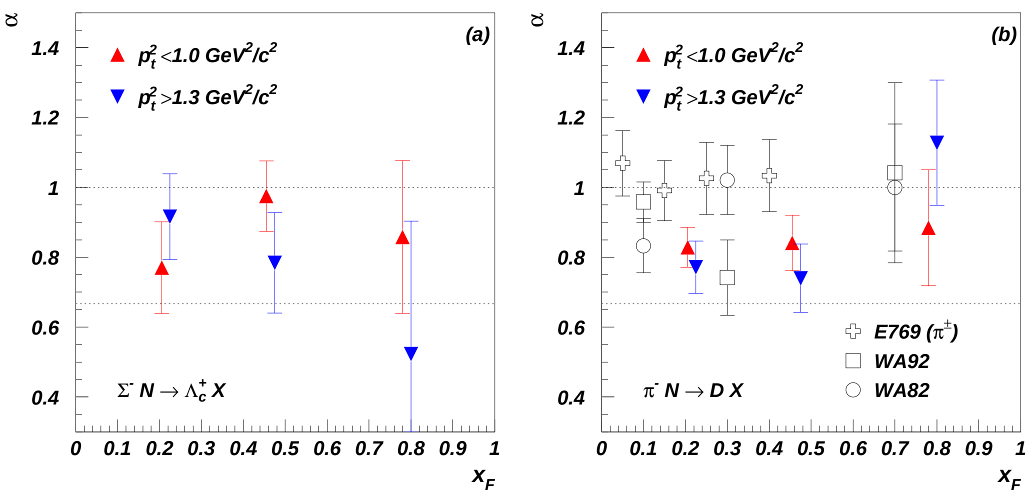

Fig. 4. α for the production of Λ_c^+ with a Σ^- (a) and for $D^{\pm}$, D^0 mesons with π^- (b) beam, as function of x_F for low ($p_t^2 < 1.0\,\mathrm{GeV}^2/c^2$) and high ($p_t^2 > 1.3\,\mathrm{GeV}^2/c^2$) transverse momentum. Our data points are slightly offset to avoid overlapping of the error bars. Reference α values of $2/3$ and 1 are shown as dotted lines. Also shown (open symbols) are results [3,4,7] from other experiments, without separation in p_t^2.

produced charm hadron carries at least one valence quark of the beam particle. Non-leading charm processes have no valence quarks in common between the beam and charm hadrons.

In Fig. 4(a) we present the dependence of α on x_F for low p_t^2 and high p_t^2 events for Λ_c^+ production by Σ^- beam events, to look for possible intrinsic charm effects [24]. Measurements of α are also available for D-meson production from the $\pi^-\,N$ experiments WA82 [3], E769 [4], and WA92 [7]. We compare our D-meson results from the π^- data to those from the other experiments in Fig. 4(b).

As a systematic check, we performed the identical analysis with Λ^0 and found good agreement with previous measurements [1,25] for both proton and Σ^- beams. Details will be presented in a forthcoming publication [26]. We looked for variations of α with any of the event selection cuts. All changes were small compared with the statistical uncertainty, indicating negligible systematic error from the cut selections. We also studied binning effects and found only small shifts, compatible with statistical uncertainties only.

5 Discussion and Conclusions

As seen from the figures, all the measured values are compatible with being independent of x_F. Averaging over all our data, we obtain $\alpha = 0.778 \pm 0.014$, which is incompatible with both usually suggested values of 2/3 and 1. Averaging separately over charm and anti-charm final states the α values show no difference (0.763 ± 0.021 and 0.791 ± 0.019).

When we separate the data into production by meson beams and that by baryon beams (Fig. 3(a)), there is a difference in the α value averaged over all charm and anti-charm modes: $\alpha_{\text{meson}} = 0.850 \pm 0.028$ for production with $\pi^\pm$ beams and $\alpha_{\text{baryon}} = 0.755 \pm 0.016$ for Σ^- and proton beams, respectively, corresponding to a $3\,\sigma$ effect. Separating into leading and non-leading production (Fig. 3(b)) we obtain $\alpha_{\text{leading}} = 0.814 \pm 0.021$ and $\alpha_{\text{nonleading}} = 0.747 \pm 0.019$, a $2.3\,\sigma$ difference.

For production of Λ_c^+ particles with a Σ^- beam the behavior shown in Fig. 4(a) seems to suggest a decrease for high x_F and p_t^2, compared to D-mesons results shown in Fig. 4(b). We note that D-meson data has only a small contribution from events with $p_t^2 > 1.3\,\text{GeV}^2/c^2$, so no firm conclusion can be drawn. All distributions are consistent with no dependence on x_F. The values of α for Λ_c^+ produced by Σ^- are 0.894 ± 0.075 and 0.841 ± 0.091, for low and high p_t^2, respectively, and for D meson produced by π^- 0.836 ± 0.045 and 0.796 ± 0.057.

In summary, within our statistics there is no dependence of α on x_F for any charm species for the interval $0.1 < x_F < 1.0$. The average value of α for charm production by pion beams is $\alpha_{\text{meson}} = 0.850 \pm 0.028$. This is somewhat larger than the corresponding average $\alpha_{\text{baryon}} = 0.755 \pm 0.016$ for charm production by baryon beams (Σ^-, p).

Acknowledgment

We thank S. Brodsky (SLAC) for useful discussions. The authors are indebted to the staff of Fermi National Accelerator Laboratory and for invaluable technical support from the staffs of collaborating institutions. This project was supported in part by Bundesministerium für Bildung, Wissenschaft, Forschung und Technologie, Consejo Nacional de Ciencia y Tecnología (CONACyT), Conselho Nacional de Desenvolvimento Científico e Tecnológico, Fondo de Apoyo a la Investigación (UASLP), Fundação de Amparo à Pesquisa do Estado de São Paulo (FAPESP), the Israel Science Foundation founded by the Israel Academy of Sciences and Humanities, Istituto Nazionale di Fisica Nucleare (INFN), the International Science Foundation (ISF), the National Science Foundation (Phy #9602178), NATO (grant CR6.941058-1360/94), the Russian Academy of Science, the Russian Ministry of Science and Technology, the Russian Foundation for Basic Research (grant 08-02-00657), the Secretaría de Educación Pública (Mexico) (grant number 2003-24-001-026), the Turkish Scientific and Technological Research Board (TÜBİTAK), and the U.S. Department of Energy (DOE grant DE-FG02-91ER40664 and DOE contract number DE-AC02-76CHO3000).

References

[1] K. J. Heller *et al.*, Phys. Rev. D **16** (1977) 2737.

[2] P. Skubic *et al.*, Phys. Rev. D **18** (1978) 3115.

[3] M. Adamovich *et al.* [WA82 Collaboration], Phys. Lett. B **284** (1992) 453.

[4] G. A. Alves *et al.* [Fermilab E769 Collaboration], Phys. Rev. Lett. **70** (1993) 722.

[5] G. A. Alves *et al.* [E769 Collaboration], Phys. Rev. D **49** (1994) 4317.

[6] M. J. Leitch *et al.* [E789 Collaboration], Phys. Rev. Lett. **72** (1994) 2542.

[7] M. Adamovich *et al.* [BEATRICE Collaboration], Nucl. Phys. B **495** (1997) 3.

[8] L. Apanasevich *et al.* [Fermilab E706 Collaboration], Phys. Rev. D **56** (1997) 1391 [arXiv:hep-ex/9702014].

[9] I. Abt *et al.* [HERA-B Collaboration], Eur. Phys. J. C **52** (2007) 531 [arXiv:0708.1443 [hep-ex]].

[10] M. J. Leitch *et al.* [FNAL E866/NuSea collaboration], Phys. Rev. Lett. **84** (2000) 3256 [arXiv:nucl-ex/9909007].

[11] B. Alessandro *et al.* [NA50 Collaboration], Eur. Phys. J. C **33** (2004) 31.

[12] I. Abt *et al.* [HERA-B Collaboration], arXiv:0812.0734 [hep-ex].

[13] H. Cobbaert *et al.* [WA78 Collaboration], Phys. Lett. B **191** (1987) 456.

[14] H. Cobbaert *et al.* [WA78 Collaboration], Phys. Lett. B **206** (1988) 546.

[15] H. Cobbaert *et al.* [WA78 Collaboration], Phys. Lett. B **213** (1988) 395.

[16] M. E. Duffy *et al.*, Phys. Rev. Lett. **55** (1985) 1816.

[17] C. Lourenco and H. K. Wohri, Phys. Rept. **433** (2006) 127 [arXiv:hep-ph/0609101].

[18] A. D. Frawley, T. Ullrich and R. Vogt, Phys. Rept. **462** (2008) 125 [arXiv:0806.1013 [nucl-ex]].

[19] J. S. Russ *et al.* [SELEX Collaboration], in *Proceedings of the 29th International Conference on High Energy Physics,* 1998, edited by A. Astbury *et al.* (World Scientific, Singapore, 1998) Vol. II, 1259 [arXiv:hep-ex/9812031].

[20] J. Engelfried *et al.*, Nucl. Instrum. Meth. A **431** (1999) 53 [arXiv:hep-ex/9811001].

[21] A. Kushnirenko *et al.* [SELEX Collaboration], Phys. Rev. Lett. **86** (2001) 5243 [arXiv:hep-ex/0010014].

[22] F. G. Garcia *et al.* [SELEX Collaboration], Phys. Lett. B **528** (2002) 49 [arXiv:hep-ex/0109017].

[23] M. Kaya *et al.* [SELEX Collaboration], Phys. Lett. B **558** (2003) 34 [arXiv:hep-ex/0302039].

[24] S. J. Brodsky, B. Kopeliovich, I. Schmidt and J. Soffer, Phys. Rev. D **73** (2006) 113005 [arXiv:hep-ph/0603238].

[25] M. I. Adamovich *et al.* [WA89 Collaboration], Eur. Phys. J. C **26** (2003) 357.

[26] A. Blanco-Covarrubias *et al.* [SELEX Collaboration], in preparation.